International Journal of Research
Available at https://edupediapublications.org/journals
p-ISSN: 2348-6848
e-ISSN: 2348-795X
Volume 03 Issue 11
July 2016

Photovoltaic Stand-Alone Scheme Based Grid Connection Applications

V.Naresh
M-tech Student Scholar
Department of Electrical & Electronics Engineering,
Mallareddy Engineering College, (Autonomous)(A)
Ranga Reddy (Dt); Telangana, India.

K.Ramesh
Asst. Professor
Department of Electrical & Electronics Engineering,
Mallareddy Engineering College, (Autonomous)(A)
Ranga Reddy (Dt); Telangana, India..

Venkateshwarlu Nailk.D
Asst. Professor
Department of Electrical & Electronics Engineering,
Mallareddy Engineering College, (Autonomous)(A)
Ranga Reddy (Dt); Telangana, India.

Abstract: In this concept PV-based stand-alone scheme for application in rural areas is proposed. Photovoltaic (PV) has become one of the most promising candidates among the available RESs. However, the availability of PV power is intermittent in nature, and hence, PV-based stand-alone systems need an energy storage element which is generally realized by utilizing a battery bank. The major challenges in designing such systems are as follows: 1) extraction of maximum power from the PV array; 2) protection of the battery from overcharge and over discharge; 3) dc to ac conversion; and 4) provision for adequate voltage boosting. As multiple objectives are required to be satisfied, the existing schemes for stand-alone systems require a minimum of three converter stages, leading to considerable reduction in the reliability and efficiency of the system. In order to address this issue, a two-stage stand-alone scheme consisting of a novel transformer coupled dual-input converter (TCDIC) followed by a conventional full-bridge inverter is proposed grid-connected photovoltaic power system, or grid-connected PV system is an electricity generating solar PV system that is connected to the utility grid. A grid-connected PV system consists of solar panels, one or several inverters, a power conditioning unit and grid connection equipment. The proposed concept is further implemented with Grid Connection based PV System simulated using Matlab/simulink software.

***Index Terms*—Battery charge control, dual-input dc–dc converter, PV-based stand-alone scheme, solar photovoltaic (PV) converter.**

I.INTRODUCTION

Nowadays demand for power throughout the world increases and these demands cannot meet by conventional sources (like thermal and hydro generation) because of limited availability of coal and water. Hence entire world foot forward to the renewable energy sources like wind and solar energy they never going to be vanish, and these are the most promising alternatives to replace conventional energy sources [1], [2]. But effective utilization of renewable sources and for getting maximum power output requires fast acting power electronic converters [3]. For three-phase applications, two types of power electronicconfigurations are commonly used to transfer power from the renewable energy resource to the grid: 1) single-stage and 2) double-stage conversion. In the doublestageconversion for a PV system, the first stage is usually a dc/dc converter and the second stage is a dc/acinverter. In first stage the DC-DC converter provides maximum power tracking from PV module and also produces appropriate DC voltage for stage-2 inversion. In stage-2 (inversion stage) inverter produces 3-øsinusoidal voltages or currents and it transfers power to load connected or to the grid.

In the case of single-stage connection, only one converter is desired to fulfill the double-stage functions, and hence the system will have a lower cost and higher efficiency, however, a more complex control method will be required. For industrial high power applications need a 3-ø system, single stage PV energy systems by using a voltage-source converter (VSC) for power conversion [4], [5]. Because of unpredictable and fluctuating nature of solar PV and wind energy systems the output of these systems not constant at terminal ends to overcome such difficultya battery storage system is employed. This also can boost the flexibility of power system control and increase the overall availability of the system [2].

High-gain multi winding transformer-based converters can be used to address this issue. However, such systems require a minimum of eight controlled switches. This is in addition to the four switches that are required to realize the inverter. Furthermore, existing stand-alone schemes employ an additional dedicated dc–dc converter to realize MPP operation. As PV power remains unavailable for more than half of a day, the utilization of this aforementioned dedicated converter becomes very poor.

A scheme wherein the use of a dedicated dc–dc converter for MPPT operation is avoided is proposed. This scheme has the PV array and battery connected in series and is designed for application in PV-powered lighting system. However, the scheme presented has the following limitations:

1) The presence of resonant elements makes the system sensitive to parameter variation;
2) Permissible variation in the duty ratio of the switches is limited within a certain range; and
3) Voltagegain is quite limited. A similar approach has also been reported for application in a grid-connected scheme.

However, the aforementioned schemes have to bypass the PV array by a diode and an inductor when PV power goes to zero.

This results in overall gain reduction as the PV and battery are connected in series.

In order to address the limitations encountered, a transformer-coupled dual-input converter (TCDIC)-based stand-alone scheme is proposed in this paper. The input stage of the proposed TCDIC is realized by connecting the PV array in series with the battery, thereby facilitating the boosting capability of the converter. The output voltage level of the TCDIC is further enhanced by incorporating a high-frequency step-up transformer. The unique feature of TCDIC is that it can be made to perform MPPT operation, battery charge control, and voltage boosting by employing a proper control algorithm.

Hence, all of the facilities that are achieved in the existing stand-alone schemes by involving two or more stages of dc–dc converters can be obtained by employing the proposed singlestage TCDIC. A standard full-bridge inverter is employed at the output of TCDIC to achieve dc–ac conversion. The basic philosophy of this scheme and its very preliminary study have been presented, and subsequently, further work that has been carried out on this scheme is presented in this paper.

II. OPERATING PRINCIPLE OF TCDIC

The schematic diagram of the TCDIC is depicted in Fig. 1. From this figure, it can be noted that no dedicated converter

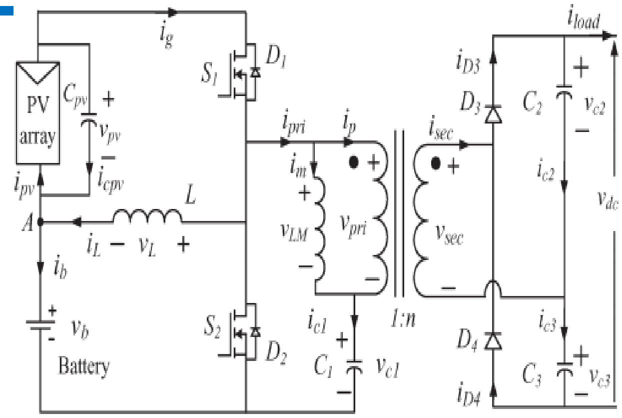

Fig. 1. Schematic circuit diagram of TCDIC.

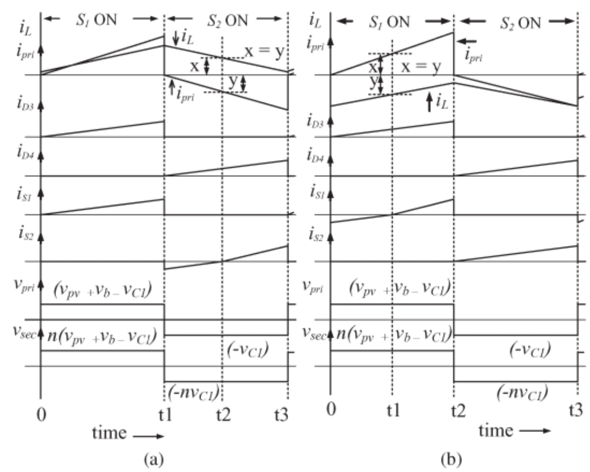

Fig. 2. Waveforms of currents flowing through and voltage across different key circuit elements of TCDIC when (a) iL is positive and (b) iL is negative.

is employed for ensuring the MPP operation of the PV array, which leads to the improved utilization of the converters involved. Furthermore, only one converter stage is present in the path between the PV array and the battery, thereby improving the charging efficiency of the battery. The inductor current iL is designed to be continuous. The switches S1 and S2 are operated in complementary fashion. All semiconductor devices and passive elements are assumed to be ideal in the following analysis.

A. Operation of the Converter When Inductor Current is Positive

The waveforms of the currents flowing through and voltages across different key circuit elements of TCDIC, while the current flowing through the inductor L is positive, are shown in Fig. 2(a). The various possible switching modes during this condition are analyzed in this section.

a) Mode I (0 to t1; S1 and D3 conducting): When S1 is turned on, the PV array voltagevpv is impressed across L,

International Journal of Research
Available at https://edupediapublications.org/journals
p-ISSN: 2348-6848
e-ISSN: 2348-795X
Volume 03 Issue 11
July 2016

and the inductor current iL increases. During this period, the voltage impressed across the primary winding of the transformer is vpri = (vpv + vb − vC1), wherein vb is the battery voltage and vC1 is the voltage across the capacitor C1. Hence, the primary current of the transformer, ipri, increases, and the capacitor C1 gets charged. The current flowing through the secondary

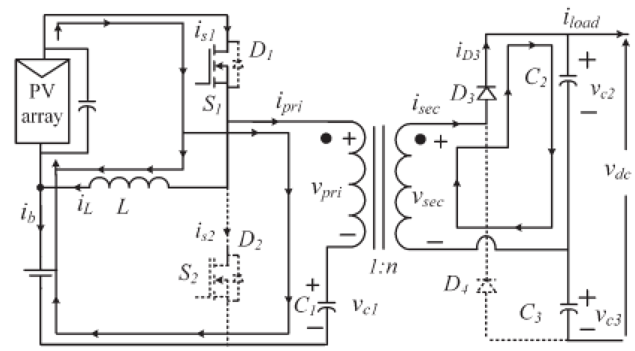

Fig. 3. Equivalent circuit diagram of TCDIC when operating in mode I and inductor current is positive.

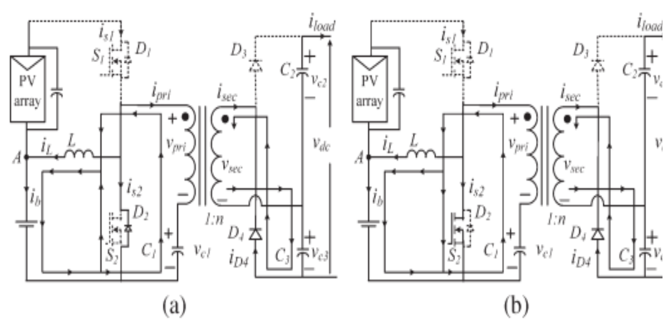

Fig. 4. Equivalent circuit diagram of TCDIC when inductor current is positive: (a) Mode II and (b) mode III.

Winding of the transformer, isec, also increases. The diode D3 is forward biased, and the capacitor C2 gets charged. The voltage across C2 is given by vC2 = n(vpv + vb − vC1), wherein n is the turns ratio of the transformer. The equivalent diagram of TCDIC during this mode is shown in Fig. 3.

b) Mode II (t1 to t2; D2 and D4 conducting): This mode begins when S1 is turned off and S2 is turned on. At the starting of this mode, iL is positive, and as S1 is turned off, ipri is zero. Since iL>ipri, the diode D2 starts conducting.

The voltage impressed across L is vL = −vb, and hence, iLstarts decreasing. The voltage impressed across the primary winding of the transformer is vpri = −vC1, and hence, ipri becomes negative and starts decreasing, thereby discharging C1. The current flowing through the secondary winding of the transformer, isec, reverses, and the diode D4 gets turned on. The capacitor C3 is getting charged, and the voltage across C3 can be expressed as vC3 = n(vC1). During this mode, iL> (−ipri) and diode D2 is forward biased. This mode continues until iLbecomes equal to (−ipri). The equivalent circuit diagram of TCDIC during this mode is shown in Fig. 4(a).

c) Mode III (t2 to t3; S2 and D4 conducting): When

iLbecomes smaller than (−ipri), the diode D2 is reverse biased, and the switch S2 starts conducting. The rest of the operation remains the same as that of mode II. The

equivalent circuit diagram of TCDIC during this mode is shown in Fig. 4(b).

B. Operation of the Converter When Inductor Current is Negative

The waveforms of the currents flowing through and voltages across different key circuit elements of TCDIC, while the current flowing through the inductor L is negative, are shown in Fig. 2(b). The various possible switching modes during thiscondition are analyzed in this section.

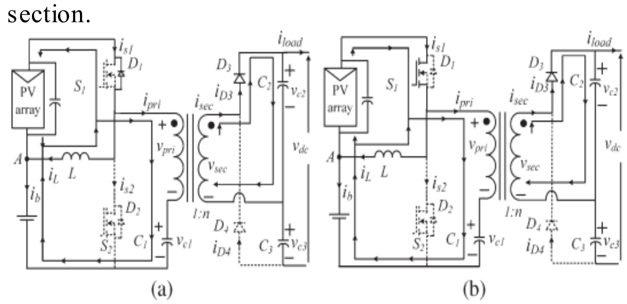

Fig. 5. Equivalent circuit diagram of TCDIC when inductor current is negative: (a) Mode I and (b) mode II.

d) Mode I (0 to t1; D1 and D3 conducting): This mode begins when S1 is turned on and S2 is turned off. At the starting of this mode, iL is negative, andipri is zero. Hence, the diode D1 starts conducting. The rest of the operation is the same as that of mode I discussed in the previous section. This mode continues until ipri becomes equal to (−iL). The equivalent circuit diagram of TCDIC during this mode is shown in Fig. 5(a).

e) Mode II (t1 to t2; S1 and D3 conducting): When ipribecomes greater than −iL, the diode D1 is reverse biased, and the switch S1 starts conducting. The rest of the operation is the same as that of mode I discussed in

International Journal of Research
Available at https://edupediapublications.org/journals
p-ISSN: 2348-6848
e-ISSN: 2348-795X
Volume 03 Issue 11
July 2016

the previous section. The equivalent circuit diagram of TCDIC during this mode is shown in Fig. 5(b).

f) Mode III (t2 to t3; S2 and D4 conducting): This mode begins when S1 is turned off and S2 is turned on. During this mode, both iL and ipri are negative, and the switch S2 conducts. The negative current in the primary winding of the transformer results in negative current in the secondary winding of the transformer. Hence, the diode D4 is forward biased, and the capacitor C3 gets charged. During operation in this mode, vL = −vb, vpri = −vC1, and vC3 = nvC1. The equivalent circuit diagram of TCDIC during this mode is the same as that show1n in Fig. 4(b), except that the direction of iL is reversed. From Fig. 1, the voltage vL across the inductor L can be expressed as

$$v_L = v_{pv}, \quad \text{when } S_1 \text{ is on}$$
$$v_L = -v_b, \quad \text{when } S_2 \text{ is on} \quad (1)$$

Therefore, the average voltage drop across the inductor is

$$V_L = DV_{pv} - (1-D)V_b$$

Wherein D is the duty ratio of the switch S1. Equating the average voltage drop across the inductor to zero,

$$V_{pv} = \left[\frac{(1-D)}{D}\right] V_b \quad (2)$$

From (2), it can be inferred that the PV voltage can be controlled by manipulating D as battery voltage Vb can be assumed to be a stiff source. Therefore, the MPPT operation of the PV array can be achieved through a proper manipulation of D. The average output voltage of the TCDIC, Vdc, is given by

$$\begin{aligned} V_{dc} &= (V_{C_2} + V_{C_3}) \\ &= [n(V_b + V_{pv} - V_{C_1}) + nV_{C_1}] \\ &= n(V_b + V_{pv}). \end{aligned} \quad (3)$$

Applying KCL at point A of Fig. 1,

$$i_L + i_{cpv} = i_b + i_{pv} \quad (4)$$

Considering the average values of iL, icpv, ib, and ipv over a switching cycle and noting that ¯ icpv = 0, (4) transforms to

$$I_b = I_L - I_{pv} \quad (5)$$

From (5), it can be noted that, for IL >Ipv, the battery is charged and, for IL <Ipv, the battery is discharged. Therefore, by controlling IL, for a given Ipv, battery charging anddischarging can be controlled. The drawback of TCDIC and the associated design constraints are presented in [23]. Thedetails of the control strategy devised for TCDIC are discussed.

IV. CONTROL STRUCTURE

The controller of a stand-alone system is required to perform the following tasks: 1) extraction of maximum power from the PV array; 2) manipulate the battery usage without violating the limits of overcharge and overdischarge; and 3) dc–ac conversion while maintaining the load voltage at the prescribed level. A controller is devised for manipulating the TCDIC to realize the first two aforementioned objectives, while the third objective is achieved by employing a conventional proportional integral (PI) controller to control the output voltage of the fullbridge inverter through sinusoidal pulse width modulation. As the conventional control scheme is used for controlling the output voltage of the inverter, its design issues are not discussed in this paper. The details of the control algorithm devised for TCDIC are presented in this section. In order to achieve the desired functionalities, TCDIC is required to operate in one of the following modes.

1) MPPT mode: Maximum power is extracted from the PV array when the system is operating in this mode. However, in order to operate in this mode, one of the following conditions must be satisfied: 1) Available maximum PV power Pmpp is more than the load demand Pl, and the surplus power can be consumed by the battery without being overcharged; and 2) Pmpp< Pl and the battery have the capability to supply Pl − Pmpp without being overdischarged. The PV power in MPPT mode is given by Ppv = Pmpp = (Pb + Pl), where Pb is the battery power which is defined as positive during charging and negative while discharging.

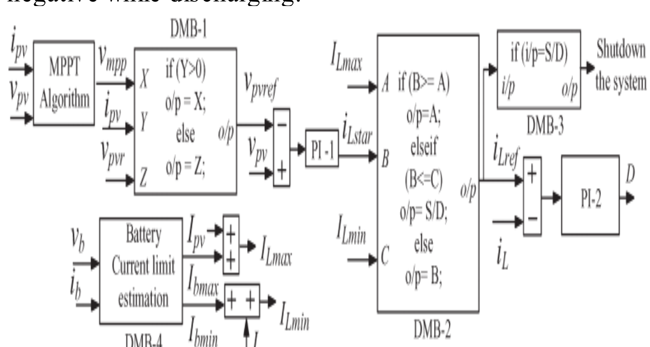

Fig. 6. Control structure for the proposed TCDIC.

2) Non-MPPT mode: Based on the state of charge (SOC) level of the battery, its charging current is required to be

limited to a maximum permissible limit Ib max to prevent the battery from getting damaged due to overcharge. The maximum charging current limit Ib max restricts the maximum power that can be absorbed by the battery to Pb max = Ib max ∗ Vb. When Pmpp> Pl and the surplus power is more than Pb max, the system cannot be operated in MPPT mode as it would overcharge the battery. During this condition, power extraction from PV is reduced to a value given by Ppv = (Pb max + Pl). This mode of operation is known as non-MPPT mode.

3) Battery only (BO) mode: The system operates in BO mode when there is no PV power and the battery has the capability to supply the load demand without being overdischarged.

4) Shutdown mode: When Pmpp< Pl and the battery does not have the capability to supply Pl − Pmpp, the system needs to be shut down to prevent the battery from being overdischarged.

The control algorithm that is employed to select the proper mode of operation for the TCDIC, depending on the status of the SOC of the battery vis-a-vis the availability of power from the solar array, is shown in Fig. 6. The proper mode selection is done by four logical decision-making blocks (DMBs). The control block DMB-1 sets the reference for the PV array voltage (Vpvref). It also decides whether the system will operate in BO mode or in MPPT mode. When it is found that ipv> 0, thereby indicating the availability of PV power, the MPPT mode of operation is selected, and the output of the MPPT algorithm block (i.e., Vmpp) sets Vpvref . When the PV power is not available, the BO mode is selected, and Vpvref is taken as Vpvr wherein Vpvr is selected so as to maintain the output voltage Vdc within the desired range of 350–460 V as per (3). The error between Vpvref and VP V is passed through a PI controller to set the required reference for the inductor current (iLstar). An upper limit IL max and a lower limit IL min is imposed on iLstar based on the relationship given in (5) to prevent overcharging and overdischarging of the battery, respectively. These two limits are derived as follows:

$$I_{L\max} = I_{b\max} + I_{pv}$$
$$I_{L\min} = I_{b\min} + I_{pv}$$

Wherein Ib max and Ib min are the maximum permissible charging and discharging current of the battery, respectively. These two limits are set based on the SOC level and the allowable depth of discharge of the battery [25]. The block DMB-4 is employed to carry out the aforementioned functions. The blockDMB-2 sets the reference level for the inductor current iLrefafter resolving the constraints imposed by IL max and IL min. When iLref remains within its prescribed limit, the system operates either in MPPT mode (for ipv> 0) or in BO mode (for ipv ≤ 0). When iLref hits its lower limit, thereby indicating that the overdischarge limit of the battery is reached, DMB-3 withdraws gating pulses from all the switches and shuts down the system. When the battery overcharging limit is attained,iLref hits its upper limit. This situation arises only when thesystem is operating in MPPT mode with Pmpp> Pl and thesurplus power is more than Pb max. In this condition, iLref is limited to IL max to limit the battery charging current to Ib max, and the MPPT is bypassed. As the battery charging current is limited to Ib max, power consumed by the battery is restricted to Pb max. This makes the available PV power more than (Pl + Pb max). This extra PV power starts charging the PV capacitor, and its voltage increases beyond Vmpp, thereby shifting the PV operating point toward the right side of the MPP point, and the power extracted from the PV array reduces. This process continues until the power drawn from the PV array becomes equal to (Pl + Pb max). Hence, during operation of the system in nonMPPT mode, the PV array is operated at a point on the right side of its true MPP, and hence, Ppv<Pmpp. If there is a decrement in load demand while operating in non-MPPT mode, power drawn from the PV array becomes more than (Pl + Pb max), and this excess power drawn starts charging the PV capacitor, thereby shifting the operating point of the PV further toward the right side of its previous operating point. In case of an increment in the load demand, the power drawn from the PV array falls short of supplying the load demand and the dc-link capacitors, and the PV capacitor starts discharging. As the voltage of the PV capacitor falls, the operating point of the PV array shifts toward the left side from its previous operating point. This leads to an increment in the power drawn from the PV array, and this process continues until the power balance is restored. In case the load demand increases to an extent such that the PV power available at its MPP falls short to supply this load, the battery will come out of its charging mode, iLref will become less than IL max, and the system operates in MPPT mode.

V.MATLAB/SIMULATION RESULTS

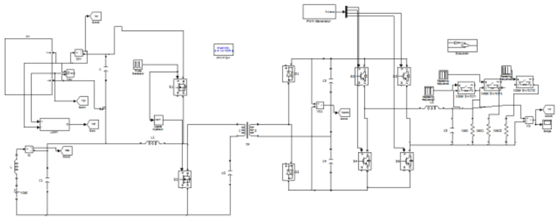

Fig 7 Matlab/simulation conventional method of Schematic of the complete stand-alone scheme.

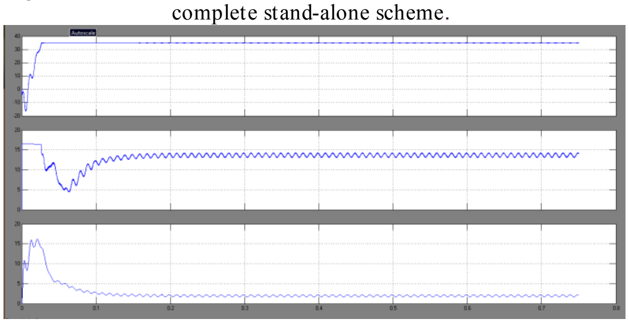

Fig 8 Simulated response of the system under steady-state operation in MPPT mode. (a) v_{pv}, i_{pv}, and i_b. (b) v_{dc} and load voltage.

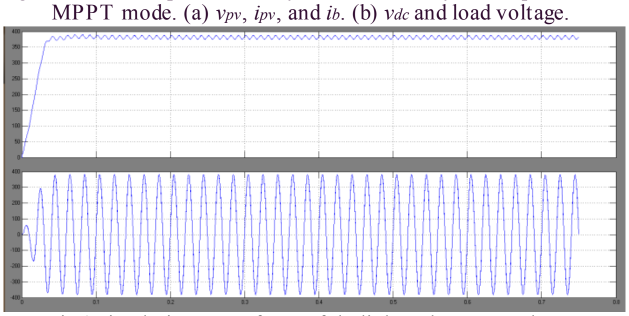

Fig 9 simulation wave form of dc-link and output voltage

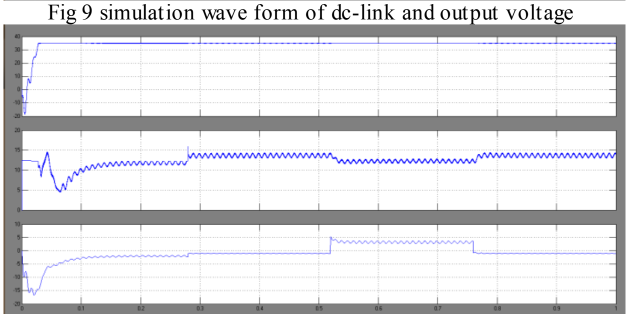

Fig 10 Simulation response of the system under steady-state operation in MPPT mode. v_{pv}, i_{pv}, and i_b. v_{dc} and load voltage.

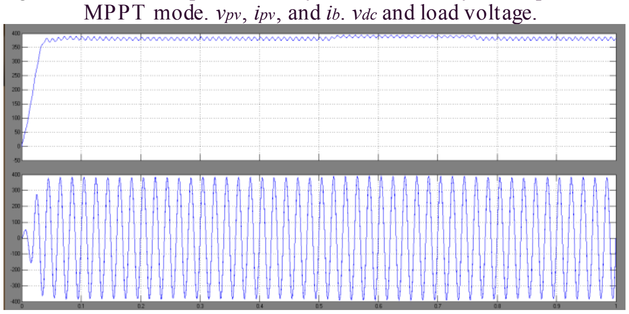

Fig 11 simulation wave form of dc-link and output voltage

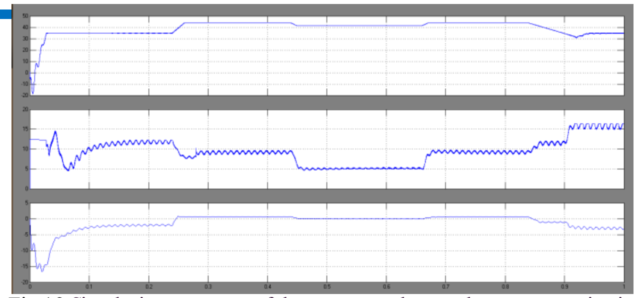

Fig 12 Simulation response of the system under steady-state operation in MPPT mode. v_{pv}, i_{pv}, and i_b. v_{dc} and load voltage.

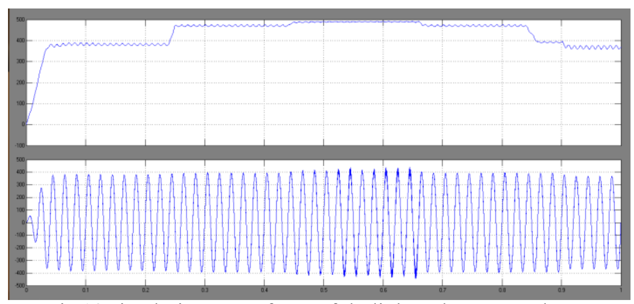

Fig 13 simulation wave form of dc-link and output voltage

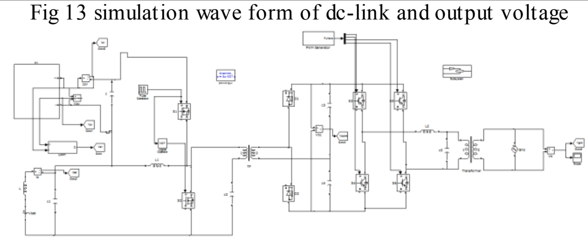

Fig 14 Matlab/simulation proposed method of Schematic of the complete grid connected system

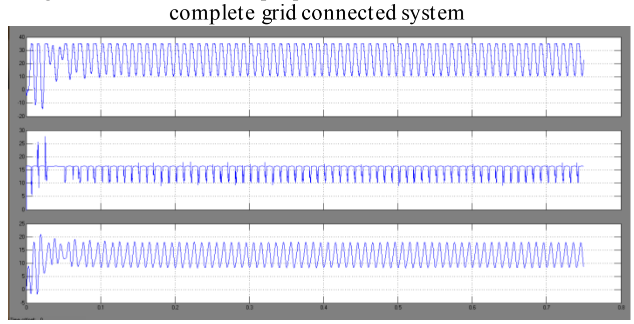

Fig 15 Simulation response of the system under steady-state operation in MPPT mode. v_{pv}, i_{pv}, and i_b. v_{dc} and load voltage in grid connected system

International Journal of Research
Available at https://edupediapublications.org/journals
p-ISSN: 2348-6848
e-ISSN: 2348-795X
Volume 03 Issue 11
July 2016

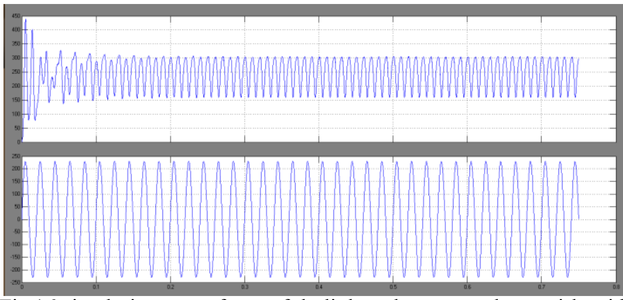

Fig 16 simulation wave form of dc-link and output voltage with grid connected system

CONCLUSION

A solar PV-based stand-alone scheme for application in rural areas is proposed in this paper. It is realized by involving a new TCDIC followed by a conventional full-bridge dc to ac inverter. A three-level NPC voltage source inverterthat can integrate both renewable energy and battery storage on the dc side of the inverter has been presented. A theoretical framework of a novel extended unbalance three-level vector modulation technique that can generate the correct ac voltage under unbalanced dc-voltage conditions has been proposed.The 3LNPC, 3L-ANPC, 3L-FC and 5L-CHB converters were compared in terms of efficiency, common mode voltage and output redundancy at nominal output current over the entire voltage variation.

REFERENCES

[1]. Hamid R. Teymour, Danny Sutanto, Kashem M. Muttaqi, and P. Ciufo, ―Solar PV and Battery Storage Integration using a New Configuration of a Three-Level NPC Inverter With Advanced Control Strategy ‖ IEEE transactions on energy conversion, vol. 29, no. 2, June, 2014.

[2]. O. M. Toledo, D. O. Filho, and A. S. A. C. Diniz,―Distributed photovoltaic generation and energy storage systems: A review,‖ Renewable Sustainable Energy, Rev., vol. 14, no. 1, pp. 506–511, 2010.

[3]. M. Bragard, N. Soltau, S. Thomas, and R. W. De Doncker, ―The balance of renewable sources and userdemands in grids: Power electronics for modular battery energy storage systems,‖ IEEE Trans. Power Electron., vol. 25, no. 12, pp. 3049–3056, Dec. 2010.

[4]. Muhammad H. Rashid, ―Power electronics circuits, devices and applications‖ Pearson education, 3rdedition, 2004.

[5]. Lewicki, Z. Krzeminski, and H. Abu-Rub, ―Spacevector pulse width modulation for three-level npc converter with the neutral point voltage control,‖ IEEE Trans. Ind. Electron., vol. 58, no. 11, pp. 5076–5086, Nov., 2011.